

Bulk and shear viscosities in lattice Boltzmann equations

Paul J. Dellar*

*Department of Applied Mathematics and Theoretical Physics,
University of Cambridge, Silver Street, Cambridge CB3 9EW, UK*

(Dated: submitted 14 Oct 2000, revised 17 May 2001, published 27th August 2001)

Lattice Boltzmann equations (LBE) are a useful tool for simulating the incompressible Navier–Stokes equations. However, LBE actually simulate a *compressible* but usually isothermal fluid at some small but finite Mach number. There has been recent interest in using LBE at larger, but still subsonic, Mach numbers, for which the viscous terms in the resulting momentum equation depart appreciably from those in the compressible Navier–Stokes equations. In particular, the isothermal constraint implies a nonzero “bulk” viscosity in addition to the usual shear viscosity. This difficulty arises at the level of the isothermal *continuum* Boltzmann equation prior to discretization. A remedy is proposed, and tested in numerical experiments with decaying sound waves. Conversely, an enhanced bulk viscosity is found useful for identifying or suppressing artifacts in under-resolved simulations of supposedly incompressible shear flows.

PACS numbers: 05.20.Dd 51.10.+y 47.11.+j

published as DOI: [10.1103/PhysRevE.64.031203](https://doi.org/10.1103/PhysRevE.64.031203)

I. INTRODUCTION

Methods based on lattice Boltzmann equations (LBE) are a promising alternative to conventional numerical methods for simulating fluid flows [1]. Lattice Boltzmann methods are straightforward to implement and have proved especially effective at simulating flows in complicated geometries, and for exploiting parallel computer architectures. They are most commonly used to simulate incompressible flows through solving the compressible, isothermal Navier–Stokes equations at small Mach numbers. The Mach number $\text{Ma} = u/c_s$ is the ratio of the fluid speed u to the sound speed c_s . When the Mach number is small, temperature and density fluctuations are $O(\text{Ma}^2)$ so the flow is approximately isothermal and incompressible.

The most common lattice Boltzmann scheme, which expands the exact Maxwell–Boltzmann equilibrium distribution to second order in Mach number and uses a Bhatnagar–Gross–Krook (BGK) approximation [2] to the collision term, contains a spurious term of $O(\text{Ma}^3)$ [3] that limits its application to small Mach number flows. The spurious term may be eliminated by expanding the equilibrium distribution to higher order in Ma and using a more complicated lattice [4, 5]. However, the viscous stresses still differ by $O(\text{Ma}^2)$ from what is normally meant by the “Navier–Stokes equations” because the bulk viscosity is nonzero. In particular, the viscous stresses differ by $O(\text{Ma}^2)$ from those calculated from the Boltzmann equation for a dilute monatomic gas. This difference is particularly relevant to recent efforts that have extended lattice Boltzmann schemes to finite, but still subsonic, Mach numbers [4, 5, 6].

In this paper we propose a modified lattice Boltzmann

scheme that allows the bulk viscosity to be adjusted, and to be set equal to zero if desired. This allows an accurate simulation of compressible flows, though still with an isothermal equation of state. An ability to adjust the bulk viscosity should also be a useful addition to non-isothermal lattice Boltzmann schemes, or for simulating materials other than dilute monatomic gases. Sterling & Chen [6] have already proposed a modified equilibrium distribution that included an adjustable effect resembling bulk viscosity. However, their deviatoric stress contained terms proportional to $\nabla\rho$. Their scheme thus approximates continuum equations that differ from the compressible Navier–Stokes equations, though they do coincide in the small Mach number limit.

The compressible Navier–Stokes equations may be written in the form

$$\partial_t \rho + \nabla \cdot (\rho \mathbf{u}) = 0, \quad (1a)$$

$$\partial_t (\rho \mathbf{u}) + \nabla \cdot (p \mathbf{I} + \rho \mathbf{u} \mathbf{u}) = \nabla \cdot \boldsymbol{\sigma}', \quad (1b)$$

where ρ , \mathbf{u} and p are the density, velocity, and thermodynamic pressure respectively. Viscous effects appear via the deviatoric stress $\boldsymbol{\sigma}'$, sometimes denoted by $\boldsymbol{\tau}$ [7], which is conventionally placed on the right hand side of (1b). In general, the pressure p is a function of the temperature θ , representing internal energy, as well as density, so the two equations above must be supplemented by an evolution equation for the temperature [8],

$$(\partial_t + \mathbf{u} \cdot \nabla) \theta + \frac{2}{3} \theta \nabla \cdot \mathbf{u} = -\nabla \cdot \mathbf{q}. \quad (2)$$

We have written $\theta = kT$, with k being Boltzmann’s constant and T the conventional temperature. The heat flux \mathbf{q} is normally taken to be $\mathbf{q} = -K \nabla \theta$, where the thermal conductivity K may depend on both ρ and θ .

On the assumptions that the deviatoric stress is linearly and isotropically related to the local velocity gradient tensor $\nabla \mathbf{u}$, and vanishes for rigid rotations, the

*Electronic address: P.J.Dellar@damtp.cam.ac.uk;
URL: <http://www.damtp.cam.ac.uk/user/pjd12>

deviatoric stress must take the generic form [7, 9, 10]

$$\sigma'_{\alpha\beta} = \mu(\partial_\alpha u_\beta + \partial_\beta u_\alpha - \frac{2}{3}\delta_{\alpha\beta}\nabla\cdot\mathbf{u}) + \mu'\delta_{\alpha\beta}\nabla\cdot\mathbf{u}. \quad (3)$$

We follow Chen & Doolen [1] in using Greek indices for vector components, reserving Roman indices for labelling discrete lattice vectors. Here μ and μ' are the first, or shear, and second, or bulk, dynamic viscosity coefficients respectively. These coefficients are material properties, and in general will be functions of the local density and temperature, but it is worth emphasising that (3) depends on the gradient of the velocity \mathbf{u} , and not on the gradient of the momentum $\rho\mathbf{u}$. Fluids for which the deviatoric stress takes this form are often called Newtonian fluids. In particular, the fluid simulated by Sterling & Chen's [6] lattice Boltzmann scheme is not a Newtonian fluid for this reason.

The topic of bulk viscosity is complicated by different authors attaching different meanings to terms like ‘‘pressure’’ and ‘‘bulk viscosity’’ [11]. We follow the conventions of Landau & Lifshitz [9], since their terminology is compatible with that normally used in the lattice Boltzmann literature. They rewrite the Navier–Stokes momentum equation (1b) in conservative form as

$$\partial_t(\rho\mathbf{u}) + \nabla\cdot\mathbf{\Pi} = 0, \quad (4)$$

where the tensor $\mathbf{\Pi} = p\mathbf{I} + \rho\mathbf{u}\mathbf{u} - \boldsymbol{\sigma}'$ is the total momentum flux. The total stress $\boldsymbol{\sigma} = -p\mathbf{I} + \boldsymbol{\sigma}'$ includes an additional isotropic contribution from the thermodynamic pressure p . The deviatoric stress is not necessarily traceless with these definitions, $\text{Tr}\boldsymbol{\sigma}' \neq 0$ in general, since the normal stress may differ from the thermodynamic pressure.

According to Landau & Lifshitz [9], the word ‘‘pressure’’ means the thermodynamic pressure, given by $p = \theta\rho$ for a perfect gas. The ‘‘bulk viscosity’’ or ‘‘second viscosity coefficient’’ multiplies any isotropic term in the deviatoric stress in addition to the traceless term present in an ideal monatomic gas. This differs from the convention used by Batchelor [12] and Lamb [13], whose ‘‘pressure’’ is the mechanical pressure, meaning minus one third the trace of the stress tensor, so the μ' term in (3) is absorbed into the ‘‘pressure.’’ Also Cercignani [14] and Tritton [7] use the term ‘‘bulk viscosity’’ for the combination $\mu' - (2/3)\mu$ that multiplies $\nabla\cdot\mathbf{u}$ in (3). Thus dilute monatomic gases ($\mu' = 0$) have negative bulk viscosity in this terminology.

To complicate matter further, expressions of the form

$$\partial_\beta\sigma'_{\alpha\beta} = \partial_\beta[\mu\partial_\beta u_\alpha + (\mu' + \mu/3)\partial_\alpha u_\beta] \quad (5)$$

sometimes appear in the literature, with the combination $\mu' + \mu/3$ labeled the ‘‘bulk viscosity’’ [5]. This is only a correct rearrangement of (3) when the combined coefficient $\mu' - 2\mu/3$ is spatially uniform, *i.e.* $\nabla(\mu' - 2\mu/3) = 0$. This holds for the particular case of an isothermal fluid using the BGK approximation with collision time $\tau \propto \rho^{-1}$, as in §V below, but does not hold in general. In the

general case, use of (5) instead of (3) implies a spurious generation of angular momentum via spatial gradients in the viscosity coefficients.

Equations (1a-b,2), with particular values for μ , μ' and K may be systematically derived from the continuum Boltzmann equation that describes a dilute gas of monatomic particles undergoing binary collisions [8, 14, 15]. This derivation employs a multiple scales expansion, the Chapman–Enskog expansion, which seeks solutions that are slowly varying on the length and timescales associated with particle collisions. However, the Navier–Stokes equations with more general forms of μ , μ' and K are often justified empirically for a much wider range of materials than dilute monatomic gases, such as liquids [7, 9, 10, 12, 13].

In particular, $\mu' = 0$ for a dilute monatomic gas, which is one justification for writing (3) in the form given, where the term proportional to the first viscosity μ has no trace. Thus a nonzero μ' implies a deviation in material properties from those of a dilute monatomic gas. Physically, a material with $\mu' = 0$ is characterised by a lack of viscous dissipation under purely isotropic expansion or contraction. We note that $\mu' \geq 0$ is required for mechanical stability. A nonzero value for μ' , along with modified values for μ and K , has been derived by Choh [16, 17] from the Bogoliubov–Born–Green–Kirkwood–Yvon (BBGKY) hierarchy which models non-dilute gases [8, 14, 17].

Lattice Boltzmann equations are usually used to simulate the incompressible Navier–Stokes equations, which follow from the compressible Navier–Stokes equations in the limit of small Mach number, $\text{Ma} = |\mathbf{u}|/c_s \rightarrow 0$, where c_s is the sound speed. If we rewrite the continuity equation (1a) to resemble the temperature equation,

$$(\partial_t + \mathbf{u}\cdot\nabla)\rho + \rho\nabla\cdot\mathbf{u} = 0. \quad (6)$$

the terms proportional to $\nabla\cdot\mathbf{u}$ in (6) and (2) are both $O(\text{Ma}^2)$. Thus an initial state with constant values ρ_0 and θ_0 will be preserved to an accuracy of $O(\text{Ma}^2)$, *i.e.* $\rho(\mathbf{x}, t) = \rho_0 + O(\text{Ma}^2)$ and $\theta(\mathbf{x}, t) = \theta_0 + O(\text{Ma}^2)$. Most lattice Boltzmann formulations in fact assume that the temperature is exactly constant, $\theta(\mathbf{x}, t) = \theta_0$, and adopt the isothermal equation of state $p = c_s^2\rho$, with constant sound speed c_s [1, 3]. Here c_s is the isothermal or Newtonian sound speed, $c_s^2 = dp/d\rho$ at constant temperature, rather than at constant entropy [13]. However, we show below that the isothermal assumption $\theta = \theta_0$ changes the form of the deviatoric stress, as well as the equation of state as intended. While this change is itself $O(\text{Ma}^2)$, it becomes relevant when lattice Boltzmann equations are used to simulate flows in the finite Mach number regime. Moreover, it appears to be significant in under-resolved lattice Boltzmann simulations of supposedly incompressible flows.

II. THE CONTINUUM BOLTZMANN EQUATION

We consider the continuum Boltzmann BGK equation [8, 14, 15, 17],

$$\partial_t f + \boldsymbol{\xi} \cdot \nabla f = -\frac{1}{\tau}(f - f^{(0)}), \quad (7)$$

where $f(\mathbf{x}, \boldsymbol{\xi}, t)$ is the single-particle distribution function, and $\boldsymbol{\xi}$ the microscopic particle velocity. The original continuum Boltzmann equation employed an integral operator on the right hand side which models binary collisions in a dilute monatomic gas. We have replaced this term by the Bhatnagar–Gross–Krook (BGK) approximation [2], in which f relaxes towards an equilibrium distribution $f^{(0)}$ with a single relaxation time τ . The Maxwell–Boltzmann equilibrium distribution in 3 dimensions is

$$f^{(0)} = \frac{\rho}{(2\pi\theta)^{3/2}} \exp\left(-\frac{(\boldsymbol{\xi} - \mathbf{u})^2}{2\theta}\right), \quad (8)$$

where ρ , \mathbf{u} and θ are the macroscopic density, velocity and temperature as above. We have scaled velocities so that the isothermal sound speed $c_s = \theta^{1/2}$. The three macroscopic quantities are defined via moments of the distribution function f ,

$$\rho = \int f d\boldsymbol{\xi}, \quad \rho \mathbf{u} = \int \boldsymbol{\xi} f d\boldsymbol{\xi}, \quad \rho \theta = \frac{1}{3} \int |\boldsymbol{\xi} - \mathbf{u}|^2 f d\boldsymbol{\xi}, \quad (9)$$

where the integrals with respect to $\boldsymbol{\xi}$ are taken over all of \mathbb{R}^3 . We observe that the equilibrium distribution $f^{(0)}$ depends on the coordinates \mathbf{x} and t only through the \mathbf{x} and t dependence of ρ , \mathbf{u} and θ .

For given ρ , \mathbf{u} and θ , the Maxwell–Boltzmann distribution is the distribution that minimises the Boltzmann entropy functional $H = \int f \ln(f) d\boldsymbol{\xi}$. The simplified BGK collision term on the right hand side of (7), like Boltzmann’s original binary collision term, drives the distribution function f towards a local Maxwell–Boltzmann equilibrium distribution $f^{(0)}$ while preserving the local density, momentum and temperature (internal energy). Thus the three moments (9) still hold if f is replaced by $f^{(0)}$. These properties are all that are required to reproduce the Navier–Stokes equations. The momentum flux tensor $\boldsymbol{\Pi}$, and the equilibrium momentum flux tensor $\boldsymbol{\Pi}^{(0)}$, are given by the complete second moment tensors of f and $f^{(0)}$ respectively,

$$\boldsymbol{\Pi} = \int \boldsymbol{\xi} \boldsymbol{\xi} f d\boldsymbol{\xi}, \quad \boldsymbol{\Pi}^{(0)} = \int \boldsymbol{\xi} \boldsymbol{\xi} f^{(0)} d\boldsymbol{\xi} = \theta \rho \mathbf{I} + \rho \mathbf{u} \mathbf{u}. \quad (10)$$

The second moment tensor is not conserved by either the BGK or the Boltzmann binary collision term. In fact, it is the difference $\boldsymbol{\sigma}' = \boldsymbol{\Pi}^{(0)} - \boldsymbol{\Pi}$ that gives rise to a deviatoric stress, and thus to viscous dissipation.

A. Chapman-Enskog expansion

The Navier–Stokes equations may be derived from moments of the continuum Boltzmann equation in the limit of

slow variations in space and time via a Chapman-Enskog expansion [8, 15, 17]. The Chapman-Enskog expansion introduces a small parameter ϵ into the collision time, so that (7) becomes

$$\partial_t f + \boldsymbol{\xi} \cdot \nabla f = -\frac{1}{\epsilon \tau}(f - f^{(0)}). \quad (11)$$

Thus spatial and temporal derivatives appear at lower order in ϵ than the collision term. The parameter ϵ may be identified physically with the dimensionless mean free path, or Knudsen number, but its purpose is to order the terms in an expansion that avoids the moment closure problem which plagues hydrodynamic turbulence. Only moments of the known equilibrium distribution $f^{(0)}$ and their derivatives in space and time are needed. In fact, ϵ may be absorbed into the collision time τ and so set equal to unity in the formulae below.

We pose a multiple scale expansion of both f and t , but not \mathbf{x} , in powers of ϵ ,

$$\begin{aligned} f &= f^{(0)} + \epsilon f^{(1)} + \epsilon^2 f^{(2)} + \dots, \\ \partial_t &= \partial_{t_0} + \epsilon \partial_{t_1} + \dots, \end{aligned} \quad (12)$$

where we may think of t_0 and t_1 as advective and diffusive (viscous) timescales respectively. We impose the two solvability conditions

$$\int f^{(n)} d\boldsymbol{\xi} = \int \boldsymbol{\xi} f^{(n)} d\boldsymbol{\xi} = 0, \quad \text{for } n = 1, 2, \dots \quad (13)$$

Thus the higher order terms $f^{(1)}, f^{(2)}, \dots$ do not contribute to the macroscopic density or momentum. These constraints, which reflect local mass and momentum conservation under collisions, lead to evolution equations for the macroscopic quantities.

Substituting the expansions (12) into the rescaled Boltzmann equation (11), we obtain

$$(\partial_{t_0} + \boldsymbol{\xi} \cdot \nabla) f^{(0)} = -\frac{1}{\tau} f^{(1)}, \quad (14a)$$

$$\partial_{t_1} f^{(0)} + (\partial_{t_0} + \boldsymbol{\xi} \cdot \nabla) f^{(1)} = -\frac{1}{\tau} f^{(2)}, \quad (14b)$$

at $O(1)$ and $O(\epsilon)$. Taking the first two moments, $\int (\cdot) d\boldsymbol{\xi}$ and $\int (\cdot) \boldsymbol{\xi} d\boldsymbol{\xi}$, of (14a) we obtain

$$\partial_{t_0} \rho + \nabla \cdot (\rho \mathbf{u}) = 0, \quad \partial_{t_0} (\rho \mathbf{u}) + \nabla \cdot \boldsymbol{\Pi}^{(0)} = 0, \quad (15)$$

where ρ , \mathbf{u} and $\boldsymbol{\Pi}^{(0)}$ are defined in (9) and (10). The right hand sides vanish by virtue of the solvability conditions (13). These two equations are equivalent to the Euler equations for an inviscid fluid, namely equations (1a,b) with $\boldsymbol{\sigma}' = 0$. Similarly, we obtain

$$\partial_{t_1} \rho = 0, \quad \partial_{t_1} (\rho \mathbf{u}) + \nabla \cdot \boldsymbol{\Pi}^{(1)} = 0, \quad (16)$$

at next order in ϵ , from the same two moments of (14b) and the solvability conditions. Neglecting terms of $O(\epsilon^2)$, equations (15) and (16) combine to give

$$\partial_t \rho + \nabla \cdot (\rho \mathbf{u}) = 0, \quad \partial_t (\rho \mathbf{u}) + \nabla \cdot (\boldsymbol{\Pi}^{(0)} + \epsilon \boldsymbol{\Pi}^{(1)}) = 0, \quad (17)$$

which are equivalent to equations (1a) and (4). The deviatoric stress $\boldsymbol{\sigma}' = -\epsilon \boldsymbol{\Pi}^{(1)}$ to this order of approximation.

An equation for the first correction stress $\boldsymbol{\Pi}^{(1)}$ follows from the second moment $\int (\cdot) \boldsymbol{\xi} \boldsymbol{\xi} d\boldsymbol{\xi}$ of (14a),

$$\partial_{t_0} \boldsymbol{\Pi}^{(0)} + \nabla \cdot \left(\int \boldsymbol{\xi} \boldsymbol{\xi} \boldsymbol{\xi} f^{(0)} d\boldsymbol{\xi} \right) = -\frac{1}{\tau} \boldsymbol{\Pi}^{(1)}. \quad (18)$$

The third moment of the equilibrium distribution $f^{(0)}$ is given by

$$\int \xi_\alpha \xi_\beta \xi_\gamma f^{(0)} d\boldsymbol{\xi} = \rho u_\alpha u_\beta u_\gamma + \theta \rho (u_\alpha \delta_{\beta\gamma} + u_\beta \delta_{\gamma\alpha} + u_\gamma \delta_{\alpha\beta}), \quad (19)$$

and we can compute $\partial_{t_0} \boldsymbol{\Pi}^{(0)}$ from the leading order time derivatives of ρ , \mathbf{u} and θ ,

$$\begin{aligned} \partial_{t_0} \Pi_{\alpha\beta}^{(0)} &= \partial_{t_0} (\theta \rho \delta_{\alpha\beta} + \rho u_\alpha u_\beta) = \partial_{t_0} (\theta \rho) \delta_{\alpha\beta} \\ &+ u_\alpha \partial_{t_0} (\rho u_\beta) + u_\beta \partial_{t_0} (\rho u_\alpha) - u_\alpha u_\beta \partial_{t_0} \rho, \end{aligned} \quad (20)$$

so (18) in fact gives an explicit expression for $\boldsymbol{\Pi}^{(1)}$ in terms of the instantaneous values of ρ , \mathbf{u} , θ and their spatial derivatives.

B. Consistent approach

In the consistent approach [8, 15], an evolution equation for the temperature θ is obtained by imposing a third solvability condition,

$$\int |\boldsymbol{\xi} - \mathbf{u}|^2 f^{(n)} d\boldsymbol{\xi} = 0, \text{ for } n = 1, 2, \dots \quad (21)$$

which reflects conservation of the internal energy $\rho\theta$ under collisions. From the trace of (18) we obtain an energy equation in the form

$$\partial_{t_0} \left(\frac{3}{2} \theta \rho + \frac{1}{2} \rho u^2 \right) + \partial_\gamma \left(\frac{1}{2} \rho u^2 u_\gamma + \frac{5}{2} \rho \theta u_\gamma \right) = -\frac{1}{2\tau} \Pi_{\alpha\alpha}^{(1)}. \quad (22)$$

The right hand side vanishes using the three solvability conditions (13) and (21) together with the identity $|\boldsymbol{\xi} - \mathbf{u}|^2 = \boldsymbol{\xi} \cdot \boldsymbol{\xi} - 2\boldsymbol{\xi} \cdot \mathbf{u} + \mathbf{u} \cdot \mathbf{u}$. The kinetic energy term $(1/2)\rho u^2$ may be eliminated using the continuity and momentum equations, leading to the internal energy equation

$$\partial_{t_0} \left(\frac{3}{2} \rho \theta \right) + \nabla \cdot \left(\frac{3}{2} \rho \theta \mathbf{u} \right) + \theta \rho \nabla \cdot \mathbf{u} = 0, \quad (23)$$

which is equivalent to the temperature equation (2) with $K = 0$, using the continuity equation (1a).

Using this new equation, along with (15), to eliminate the time derivatives ∂_{t_0} in (20), we obtain [8, 15]

$$\Pi_{\alpha\beta}^{(1)} = -\tau \theta \left(\partial_\alpha u_\beta + \partial_\beta u_\alpha - \frac{2}{3} \delta_{\alpha\beta} \nabla \cdot \mathbf{u} \right). \quad (24)$$

Thus the deviatoric stress $\boldsymbol{\sigma}' = -\epsilon \boldsymbol{\Pi}^{(1)}$, is of the form (3) with $\mu = \epsilon \tau \theta$ and $\mu' = 0$. The absence of the second viscous effect, or the fact that $\text{Tr } \boldsymbol{\sigma}' = 0$, is a direct consequence of internal energy conservation under collisions, as expressed by the temperature solvability condition (21).

An equation for $\partial_{t_1} \theta$, where thermal conduction appears, may be found from the $|\boldsymbol{\xi} - \mathbf{u}|^2$ moment of (14b). The additional term takes the expected form $\mathbf{q} = -K \nabla \theta$, where $K = (5/2)\mu = (5/2)\rho \theta \tau$ for the BGK approximation.

C. Isothermal approximation

As discussed in the Introduction, most lattice Boltzmann formulations take the temperature to be exactly constant, $\theta = \theta_0$, rather than allowing it to vary by $O(\text{Ma}^2)$ in response to a nonzero divergence $\nabla \cdot \mathbf{u}$. Thus the solvability condition (21) for the temperature, which in fact represents conservation of energy under collisions, is replaced by the constrain $\theta = \theta_0$.

In this case the terms arising from $\partial_{t_0} \theta$ and $\nabla \theta$ in the earlier calculation are missing, so now (18) simplifies to [3, 18, 19]

$$\Pi_{\alpha\beta}^{(1)} = -\tau \theta \rho (\partial_\alpha u_\beta + \partial_\beta u_\alpha). \quad (25)$$

The deviatoric stress $\boldsymbol{\sigma}' = -\epsilon \boldsymbol{\Pi}^{(1)}$ is still of the form (3) with first viscosity coefficient $\mu = \epsilon \tau \rho \theta$ as before, but now there is a nonzero second viscosity coefficient $\mu' = (2/3)\mu$.

By direct calculation, $\text{Tr } \boldsymbol{\Pi}^{(1)} = -2\tau \theta \rho \nabla \cdot \mathbf{u}$, so the analogue of (23) acquires a nonzero right hand side,

$$\partial_{t_0} \left(\frac{3}{2} \rho \theta \right) + \nabla \cdot \left(\frac{3}{2} \rho \theta \mathbf{u} \right) + \theta \rho \nabla \cdot \mathbf{u} = -\frac{1}{2\tau} \text{Tr } \boldsymbol{\Pi}^{(1)}, \quad (26)$$

which exactly cancels the $\theta \rho \nabla \cdot \mathbf{u}$ forcing term. The internal energy equation is now exactly satisfied by θ being constant, since it then coincides with the continuity equation (1a).

III. FROM CONTINUUM BOLTZMANN TO LATTICE BOLTZMANN

Although lattice Boltzmann equations were first constructed as empirical extensions of the earlier lattice gas automata (LGA) [20] to continuous distribution functions [21, 22], they may also be derived systematically by truncating the continuum Boltzmann equation in velocity space [23, 24, 25, 26]. This derivation determines several otherwise arbitrary constants in the construction [18, 26]. A lattice Boltzmann equation with a Coriolis force also arises naturally from the analogous derivation in a rotating frame [19].

As lattice Boltzmann equations are normally used to simulate fluids at low Mach numbers, it is usual to exploit

the small Mach number to expand the exact equilibrium distribution $f^{(0)}$ up to second order in the macroscopic velocity \mathbf{u} . Recall that we have scaled velocities so that $c_s = \theta^{1/2}$ is $O(1)$ so $|\mathbf{u}| = O(\text{Ma}) \ll 1$. We replace the exact Maxwell–Boltzmann distribution (8) by

$$f^{(0)} = \rho w(\boldsymbol{\xi}) \left(1 + \frac{\boldsymbol{\xi} \cdot \mathbf{u}}{\theta} + \frac{(\boldsymbol{\xi} \cdot \mathbf{u})^2}{2\theta^2} - \frac{\mathbf{u}^2}{2\theta} \right) + O(\mathbf{u}^3), \quad (27)$$

where $w(\boldsymbol{\xi})$ is the weight function

$$w(\boldsymbol{\xi}) = (2\pi\theta)^{-3/2} \exp(-\boldsymbol{\xi}^2/2\theta). \quad (28)$$

The $\rho\mathbf{u}\mathbf{u}\mathbf{u}$ term in the exact third moment $\int \boldsymbol{\xi}\boldsymbol{\xi}\boldsymbol{\xi}f^{(0)}d\boldsymbol{\xi}$ as calculated in (19) above disappears when $f^{(0)}$ is replaced by its truncated form (27). Thus the two deviatoric stresses calculated above each acquire an extra term $-\tau\nabla \cdot (\rho\mathbf{u}\mathbf{u}\mathbf{u})$ [3]. Since this extra term is $O(\text{Ma}^3)$ it only becomes appreciable in the finite Mach number regime [5].

With the expanded form (27) of the equilibrium distribution $f^{(0)}$, the integrals appearing in equations (9), (10) and (19) are all of the form

$$\int p_n(\boldsymbol{\xi})w(\boldsymbol{\xi})d\boldsymbol{\xi}, \quad 0 \leq n \leq 5, \quad (29)$$

where $p_n(\boldsymbol{\xi})$ denotes a polynomial of degree n in the components of $\boldsymbol{\xi}$. He & Luo [23, 24] realised, in the context of lattice Boltzmann equations, that these integrals may be evaluated as sums using Gaussian quadrature formulae,

$$\int p_n(\boldsymbol{\xi})w(\boldsymbol{\xi})d\boldsymbol{\xi} = \sum_{i=0}^N w_i p_n(\boldsymbol{\xi}_i). \quad (30)$$

The points $\boldsymbol{\xi}_i$ are known as quadrature points, and the coefficients w_i are the corresponding weights [27]. The number N of quadrature points required depends on the maximum degree n of the polynomial, and the dimension D of the $\boldsymbol{\xi}$ space.

Only the values of the distribution function as evaluated at the quadrature points $\boldsymbol{\xi}_i$ need be evolved in \mathbf{x} and t , since these values are sufficient to evaluate the required moments using (30). Thus the continuum Boltzmann equation (7) may be replaced by the lattice Boltzmann equation,

$$\partial_t f_i + \boldsymbol{\xi}_i \cdot \nabla f_i = -\frac{1}{\tau}(f_i - f_i^{(0)}), \quad \text{for } i = 0, \dots, N, \quad (31)$$

where $f_i(\mathbf{x}, t) = w_i f(\mathbf{x}, \boldsymbol{\xi}_i, t)/w(\boldsymbol{\xi}_i)$ (compare equations (27) and (35)), and the macroscopic quantities of density, momentum, and momentum flux are now given by

$$\rho = \sum_{i=0}^N f_i, \quad \rho\mathbf{u} = \sum_{i=0}^N \boldsymbol{\xi}_i f_i, \quad \boldsymbol{\Pi} = \sum_{i=0}^N \boldsymbol{\xi}_i \boldsymbol{\xi}_i f_i. \quad (32)$$

A. Two dimensional, nine speed lattice Boltzmann equation

The most common quadrature formula in two dimensions ($D = 2$) uses nine quadrature points, leading to the so-called nine speed lattice Boltzmann model [1, 3, 18]. If we take the temperature $\theta = 1/3$, the quadrature points lie on an integer lattice,

$$\boldsymbol{\xi}_i = \begin{cases} (0, 0), & i=0, \\ (\sin((i-1)\pi/2), \cos((i-1)\pi/2)), & i=1,2,3,4, \\ \sqrt{2}(\sin((2i-1)\pi/4), \cos((2i-1)\pi/4)), & i=5,6,7,8. \end{cases} \quad (33)$$

The corresponding weight factors are

$$w_i = \begin{cases} 4/9, & i=0, \\ 1/9, & i=1,2,3,4, \\ 1/36, & i=5,6,7,8, \end{cases} \quad (34)$$

and the discrete equilibrium distributions functions are

$$f_i^{(0)} = w_i \rho \left(1 + 3\boldsymbol{\xi}_i \cdot \mathbf{u} + \frac{9}{2}(\boldsymbol{\xi}_i \cdot \mathbf{u})^2 - \frac{3}{2}\mathbf{u}^2 \right). \quad (35)$$

Although the results follow from the construction via Gaussian quadratures, the required moments may be evaluated directly with the aid of identities such as [18]

$$\sum_{i=0}^8 w_i \boldsymbol{\xi}_i = 0, \quad \sum_{i=0}^8 w_i \boldsymbol{\xi}_i \boldsymbol{\xi}_i = \frac{1}{3}\mathbf{I}, \quad \sum_{i=0}^8 w_i \boldsymbol{\xi}_i \boldsymbol{\xi}_i \boldsymbol{\xi}_i = 0. \quad (36)$$

IV. FULLY DISCRETE LATTICE BOLTZMANN EQUATION

To achieve a fully discrete lattice Boltzmann equation we must approximate (31) in \mathbf{x} and t . Integrating (31) along a characteristic for a time interval Δt , we obtain

$$f_i(\mathbf{x} + \boldsymbol{\xi}_i \Delta t, t + \Delta t) - f_i(\mathbf{x}, t) = -\frac{1}{\tau} \int_0^{\Delta t} f_i(\mathbf{x} + \boldsymbol{\xi}_i s, t + s) - f_i^{(0)}(\mathbf{x} + \boldsymbol{\xi}_i s, t + s) ds. \quad (37)$$

The integral may be approximated by the trapezium rule with second order accuracy, thus

$$f_i(\mathbf{x} + \boldsymbol{\xi}_i \Delta t, t + \Delta t) - f_i(\mathbf{x}, t) = -\frac{\Delta t}{2\tau} \left(f_i(\mathbf{x} + \boldsymbol{\xi}_i \Delta t, t + \Delta t) - f_i^{(0)}(\mathbf{x} + \boldsymbol{\xi}_i \Delta t, t + \Delta t) + f_i(\mathbf{x}, t) - f_i^{(0)}(\mathbf{x}, t) \right) + O(\Delta t^3). \quad (38)$$

Unfortunately, $f_i^{(0)}(\mathbf{x} + \boldsymbol{\xi}_i \Delta t, t + \Delta t)$ is not known independently of the set $f_i(\mathbf{x} + \boldsymbol{\xi}_i \Delta t, t + \Delta t)$, so (38) appears to yield a system of coupled nonlinear algebraic equations for the f_i at time $t + \Delta t$. However, the system may be

rendered fully explicit by a change of variables [19, 28]. Introducing a different set of distribution functions \bar{f}_i defined by

$$\bar{f}_i(\mathbf{x}, t) = f_i(\mathbf{x}, t) + \frac{\Delta t}{2\tau} \left(f_i(\mathbf{x}, t) - f_i^{(0)}(\mathbf{x}, t) \right), \quad (39)$$

the above scheme (38) is algebraically equivalent to the fully explicit scheme

$$\begin{aligned} & \bar{f}_i(\mathbf{x} + \boldsymbol{\xi}\Delta t, t + \Delta t) - \bar{f}_i(\mathbf{x}, t) = \\ & - \frac{\Delta t}{\tau + \Delta t/2} \left(\bar{f}_i(\mathbf{x}, t) - f_i^{(0)}(\mathbf{x}, t) \right). \end{aligned} \quad (40)$$

The macroscopic density, momentum, and momentum flux are readily reconstructed from moments of the \bar{f}_i ,

$$\begin{aligned} \rho &= \sum_{i=0}^N \bar{f}_i, \quad \rho \mathbf{u} = \sum_{i=0}^N \boldsymbol{\xi}_i \bar{f}_i, \\ \left(1 + \frac{\Delta t}{2\tau} \right) \boldsymbol{\Pi} &= \sum_{i=0}^N \boldsymbol{\xi}_i \boldsymbol{\xi}_i \bar{f}_i + \frac{\Delta t}{2\tau} \boldsymbol{\Pi}^{(0)}. \end{aligned} \quad (41)$$

This formulation is equivalent to the usual construction based on a Taylor expansion of the discrete equation (40) which observes that second order accuracy may be achieved with what looks like only a first order approximation to (31), by replacing the relaxation time τ with $\tau + \Delta t/2$ [1]. However, the variables often denoted f_i appearing in the discrete system are actually the \bar{f}_i in our notation, so the non-equilibrium momentum flux $\boldsymbol{\Pi}^{(1)}$ in the fully discrete system (40) is given by

$$\boldsymbol{\Pi}^{(1)} = \frac{\bar{\boldsymbol{\Pi}} - \boldsymbol{\Pi}^{(0)}}{1 + \Delta t/(2\tau)}, \quad (42)$$

rather than by $\boldsymbol{\Pi} - \boldsymbol{\Pi}^{(0)}$ as in the continuous system.

V. DENSITY DEPENDENT VISCOSITIES

If the Chapman–Enskog analysis of §II is applied to the Boltzmann equation with Boltzmann’s original binary collision operator instead of the BGK approximation, we find that the dynamic viscosity μ is independent of density, and a function of temperature only. This surprising result, subsequently verified experimentally, was one of the first successes of classical kinetic theory [17]. To reproduce this using the BGK approximation it is necessary to make the collision timescale τ inversely proportional to the local density, $\tau \propto \rho^{-1}$, and thus a function of position. The analysis of §IV is unchanged, apart from τ being a function $\tau(\mathbf{x}, t)$ instead of a constant.

VI. ADJUSTABLE BULK VISCOSITY

We modify the bulk viscosity coefficient in the isothermal lattice Boltzmann equation by redefining the equi-

librium distribution functions to be

$$\begin{aligned} f_i^{(0)} &= \rho w_i \left(1 + \frac{\boldsymbol{\xi} \cdot \mathbf{u}}{\theta} + \frac{(\boldsymbol{\xi} \cdot \mathbf{u})^2}{2\theta^2} - \frac{|\mathbf{u}|^2}{2\theta} \right) \\ &+ w_i \left(\frac{\mu'}{2\mu} - \frac{1}{3} \right) \frac{(|\boldsymbol{\xi}_i|^2 - D\theta)}{2\theta^2} (\text{Tr } \boldsymbol{\Pi}^{(1)}). \end{aligned} \quad (43)$$

The number of spatial dimensions is D , which appears via $\text{Tr } \mathbf{I} = D$. These $f_i^{(0)}$ are functions of $\{f_1, \dots, f_N\}$ through \mathbf{u} and ρ as before, and now also through $\text{Tr } \boldsymbol{\Pi}^{(1)}$ as calculated in (46) below. The 1, $\boldsymbol{\xi}$, and $\boldsymbol{\xi}\boldsymbol{\xi}\boldsymbol{\xi}$ moments of (43) are unchanged, while the $\boldsymbol{\xi}\boldsymbol{\xi}$ moment becomes

$$\boldsymbol{\Pi}^{(0)} = \theta \rho \mathbf{I} + \rho \mathbf{u} \mathbf{u} + \left(\frac{\mu'}{2\mu} - \frac{1}{3} \right) (\text{Tr } \boldsymbol{\Pi}^{(1)}) \mathbf{I}. \quad (44)$$

Since $\text{Tr } \boldsymbol{\Pi}^{(1)} = -2\theta\rho\tau\nabla \cdot \mathbf{u}$ from (25), the combined momentum flux tensor becomes

$$\boldsymbol{\Pi} = \boldsymbol{\Pi}^{(0)} + \boldsymbol{\Pi}^{(1)} = \theta\rho\mathbf{I} + \rho\mathbf{u}\mathbf{u} - \boldsymbol{\sigma}', \quad (45)$$

where $\boldsymbol{\sigma}'$ is the full deviatoric stress as in (3). The ratio μ'/μ appearing in (43) may be an arbitrary function of the local density ρ .

As $\text{Tr } \boldsymbol{\Pi}^{(0)}$ itself depends on $\text{Tr } \boldsymbol{\Pi}^{(1)}$ via (44), the trace of equation (42) rearranges to give

$$\left[1 + \frac{\Delta t}{2\tau} + D \left(\frac{\mu'}{2\mu} - \frac{1}{3} \right) \right] \text{Tr } \boldsymbol{\Pi}^{(1)} = \text{Tr } \bar{\boldsymbol{\Pi}} - D\theta\rho - \rho u^2, \quad (46)$$

which is the expression we used in conjunction with (43) to compute $f_i^{(0)}$ in terms of \bar{f}_i . We note that in three dimensions with no bulk viscosity, $D = 3$ and $\mu' = 0$, the coefficient on the left hand side of (46) is saved from vanishing by the $\Delta t/(2\tau)$ term. Thus it is possible to simulate flows with $\text{Tr } \boldsymbol{\sigma}' = 0$ using this scheme.

This alteration to the equilibrium stress $\boldsymbol{\Pi}^{(0)}$ also changes the perturbation stress $\boldsymbol{\Pi}^{(1)}$, because equation (18) for $\boldsymbol{\Pi}^{(1)}$ contains the term $-\tau\partial_{t_0}\boldsymbol{\Pi}^{(0)}$. However, the new term in $\boldsymbol{\Pi}^{(0)}$ is only $O(\tau)$, one order smaller than the other terms, so the new term in $\boldsymbol{\Pi}^{(1)}$ is $O(\tau^2)$. This new term is also one order smaller than the other terms in $\boldsymbol{\Pi}^{(1)}$, and is thus comparable with the so-called Burnett terms involving $f_i^{(2)}$ that arise at higher order in the Chapman–Enskog expansion of the continuum Boltzmann equation [14, 15]. Since we aim to recover the Navier–Stokes equations with modified bulk viscosity by truncating the Chapman–Enskog expansion at $O(\tau)$, it is consistent to neglect both $\boldsymbol{\Pi}^{(2)}$ and the new $\tau^2\partial_{t_0}\nabla \cdot \mathbf{u}$ term in $\boldsymbol{\Pi}^{(1)}$. We show in §VII below that deviations from the intended Navier–Stokes behaviour at finite τ are no worse than for the unmodified lattice Boltzmann equation.

VII. NUMERICAL EXPERIMENTS

We performed numerical experiments to measure the bulk viscosity of the two dimensional nine speed lattice

Boltzmann model with the modified equilibrium distribution appearing in (43). We also investigated the effect of varying bulk viscosity on a nominally incompressible but under-resolved simulation of a Kelvin–Helmholtz instability. Both sets of experiments were performed using periodic boundary conditions.

A. Sound waves

We measured the bulk viscosity from the rate of decay of sound waves in numerical experiments. For flows of the form $\rho = \rho_0 + \rho'(x, t)$ and $\mathbf{u} = u'(x, t)\hat{\mathbf{x}}$, with ρ' and u' both small, the linearised form of the Navier–Stokes equations (1a,b) that govern sound waves may be reduced to [13]

$$\partial_{tt}u = c_s^2 \partial_{xx}u + \left(\frac{4}{3}\nu + \nu'\right) \partial_{xxt}u, \quad (47)$$

where $\nu = \mu/\rho_0$ and $\nu' = \mu'/\rho_0$ are the kinematic shear and bulk viscosities respectively. This equation has solutions of the form $u(x, t) \propto \exp(ikx + \sigma t)$ provided σ satisfies the dispersion relation [13]

$$\sigma = -\left(\frac{2}{3}\nu + \frac{1}{2}\nu'\right)k^2 \pm ikc_s \left[1 - \left(\frac{4}{3}\nu + \nu'\right)\frac{k^2}{c_s^2}\right]^{1/2}. \quad (48)$$

For small amplitude waves the nonlinear terms present in the lattice Boltzmann simulation are negligible, including the $O(\text{Ma}^3)$ nonlinear correction $\nabla \cdot (\rho \mathbf{u} \mathbf{u} \mathbf{u})$ to the deviatoric stress. This was verified by observing that the numerical solutions decayed exponentially as predicted by the linear theory. Sound waves in a hexagonal six speed lattice Boltzmann scheme were studied previously in [29], but with an emphasis on nonlinear steepening at finite amplitude.

Viscous dissipation of sound waves depends upon the combination $\tilde{\nu} = (4/3)\nu + \nu'$ of the shear and bulk viscosities, which we refer to as the effective viscosity. In Fig. 1 we plot the ratio $\tilde{\nu}_m/\tilde{\nu}$ of the measured effective viscosity $\tilde{\nu}_m$ to its intended value $\tilde{\nu}$, for varying $\tilde{\nu}$ and several fixed ratios ν'/ν of bulk to shear viscosities. The measured values were computed from the decay of the energy $E(t) = u^2 + c_s^2 \rho'^2$ by a least squares fit of a straight line to the logarithm $\ln E(t)$. The energy in fact decays in an oscillatory fashion, because viscous dissipation is proportional to the oscillatory instantaneous fluid velocity, but a simple straight line fit proved adequate. The initial conditions were $u = 0$ and $\rho = 1 + 10^{-6} \sin(2\pi x)$, using 64 lattice points. Simulations with larger values of $\tilde{\nu}$ used 128 bit arithmetic, with approximately 33 significant digits, so more oscillations could be followed before the sound wave decayed to the level of numerical round-off error.

The independent variable in Fig. 1 is the Knudsen number $\text{Kn} = \text{Ma}/\text{Re} = \tau/\sqrt{3}$. Introducing dimensionless variables in which the simulation domain is of length

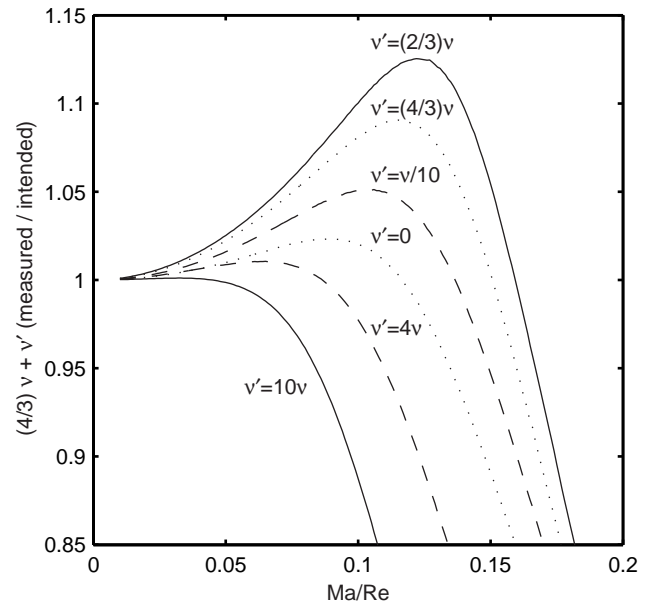


FIG. 1: Ratio of measured to intended effective viscosity $(4/3)\nu + \nu'$ for sound waves, plotted against Knudsen number $\text{Kn} = \text{Ma}/\text{Re} = \tau/\sqrt{3}$. The unmodified 9 speed lattice Boltzmann scheme is equivalent to $\nu' = (2/3)\nu$ (uppermost solid line).

1, it is convenient to choose the time unit so that a typical fluid velocity is of magnitude 1. The sound speed is then $1/\text{Ma}$, and the particle speeds are $\sqrt{3}/\text{Ma}$ or $\sqrt{6}/\text{Ma}$. The Reynolds number is defined as $\text{Re} = 1/\tilde{\nu}$, using the effective viscosity and unit length and velocity scales, so $\text{Ma}/\text{Re} = \tilde{\nu}/c_s$.

The measured effective viscosities are close to their intended values, indicated by $\tilde{\nu}_m/\tilde{\nu} \approx 1$ in Fig. 1, for various values of the ratio ν'/ν provided the Knudsen number is not too large, in the sense that $\text{Ma}/\text{Re} < 0.03$ for a 1% error, and $\text{Ma}/\text{Re} < 0.01$ for a 0.1% error. The curve $\nu' = (2/3)\nu$ corresponds to the unmodified nine speed lattice Boltzmann scheme, so the deviations introduced by the modified bulk viscosity at finite Knudsen number are no worse than those already present.

The curves in Fig. 1 are all parabolic for small τ . Since we have divided by τ in computing the ratio of the measured to intended decay rate, this implies that the deviations in the measured decay rate are due to the super-Burnett corrections at $O(\tau^3)$ in the Chapman–Enskog expansion [15]. This is confirmed analytically in the appendix. The Burnett correction at $O(\tau^2)$, the first correction beyond Navier–Stokes, is dispersive and so only alters the frequency, not the decay rate. This correction has been found by Qian & Zhou [30] for the unmodified 9 speed lattice Boltzmann scheme. It differs from the Burnett correction to the continuum Boltzmann equation because the ξ^4 moment of the truncated equilibrium (27) differs from the ξ^4 of the original Maxwell–Boltzmann equilibrium (8).

For the purposes of simulating nearly incompressible

flows, the lattice Boltzmann scheme may be made accurate for arbitrarily large $\bar{\nu}$, corresponding to arbitrarily small Reynolds numbers, by making the Mach number sufficiently small. This is equivalent to taking sufficiently small timesteps, by comparison with the timescale set by the fluid velocity and the lattice spacing, but not by comparison with the timescale of evolving sound waves. Demonstrating correct viscous dissipation of sound waves is thus quite a strenuous test because the lattice Boltzmann scheme is intended to simulate motions that evolve on timescales much longer than the periods of sound waves.

B. Doubly periodic shear layers

Minion & Brown [31] studied the performance of various numerical schemes in under-resolved simulations of the 2D incompressible Navier–Stokes equations. Their initial conditions corresponded to a perturbed shear layer,

$$u_x = \begin{cases} \tanh(k(y - 1/4)), & y \leq 1/2, \\ \tanh(k(3/4 - y)), & y > 1/2, \end{cases} \quad (49)$$

$$u_y = \delta \sin(2\pi(x + 1/4)),$$

in the doubly periodic domain $0 \leq x, y \leq 1$. The parameter k controls the width of the shear layers, and δ the magnitude of the initial perturbation. The shear layer is expected to roll up due to a Kelvin–Helmholtz instability excited by the $O(\delta)$ perturbation in u_y . With $k = 80$, $\delta = 0.05$, and a Reynolds number $\text{Re} = \nu^{-1} = 10000$, the thinning shear layer between the two rolling up vortices becomes under-resolved on a 128×128 grid. Minion & Brown [31] found that conventional numerical schemes using centred differences became unstable for this under-resolved flow, whereas the “robust” or “upwind” schemes that actively suppress grid-scale oscillations all produced two spurious secondary vortices at the thinnest points of the two shear layers.

Fig. 2 shows that two spurious vortices are generated by the 9 speed lattice Boltzmann equation with unmodified bulk viscosity. The vorticity $\omega = \partial_x u_y - \partial_y u_x$ was computed from the velocities u_x and u_y at grid points by spectrally accurate differentiation. The shear layers become under-resolved at $t = 0.6$, see top of Fig. 3, due to stretching as the two large vortices roll up. This stretching is associated with a nonzero numerical divergence, $\nabla \cdot \mathbf{u} \neq 0$, at the two halfway points where the spurious vortices form, as shown in the lower half of Fig. 3. The numerical divergence is due to a lack of spatial resolution, and not to an insufficiently small Mach number, since it was almost unchanged by reducing the Mach number from 0.04 to 0.01. Moreover, the divergence computed from $\text{Tr } \mathbf{\Pi}^{(1)}$ was almost indistinguishable from that computed by spectrally differentiating u_x and u_y .

Fig. 4 shows that removing the bulk viscosity, $\mu' = 0$, increases the strength of the spurious vortices compared

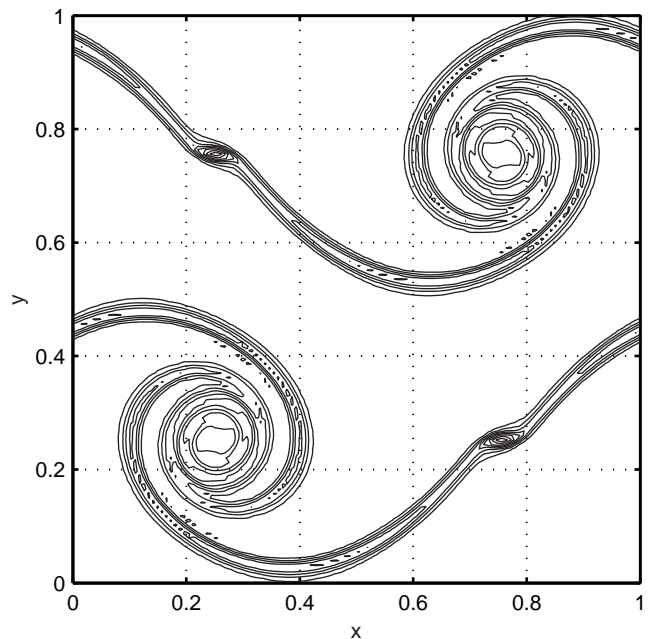


FIG. 2: Contours of vorticity at $t = 1$ from the unmodified 9 speed lattice Boltzmann equation on a 128×128 grid with $\text{Ma} = 0.04$ and $\text{Re} = 10000$. Compare Fig. 8 in [31]. The contour interval is $\Delta\omega = 6$.

with the unmodified lattice Boltzmann equation. Conversely, enhancing the bulk viscosity to $\mu' = 10\mu$ successfully prevents the formation of spurious vortices as shown in Fig. 5. Increasing the bulk viscosity further to $\mu' = 100\mu$ produced no further visible changes. This is all consistent with the spurious vortices being caused by an apparent divergence in the thin shear layers when they become too narrow to be resolved by the grid. The enhanced bulk viscosity acts to smooth out the flow at just those points where there is an apparent divergence, but leaves the rest of the flow almost unaffected.

In a well-resolved 256×256 simulations the vorticity was independent of the bulk viscosity, with a fractional variation of 10^{-6} for $0 \leq \mu'/\mu \leq 100$, and showed the expected second order convergence in Mach number based on simulations with $\text{Ma} = 0.01, 0.02$, and 0.04 . Although there was still some discrepancy in the two main vortices between the 128×128 simulations with enhanced bulk viscosity and the 256×256 simulations, most likely due to a slight shift in position of the vortex filaments, the discrepancy in the stretched shear layers was almost entirely eliminated.

VIII. CONCLUSION

The usual derivation of lattice Boltzmann equations involves replacing the temperature evolution equation in the Chapman–Enskog expansion by an isothermal assumption. This introduces a bulk viscosity $\mu' = 2\mu/3$ into the deviatoric stress that is not present with a con-

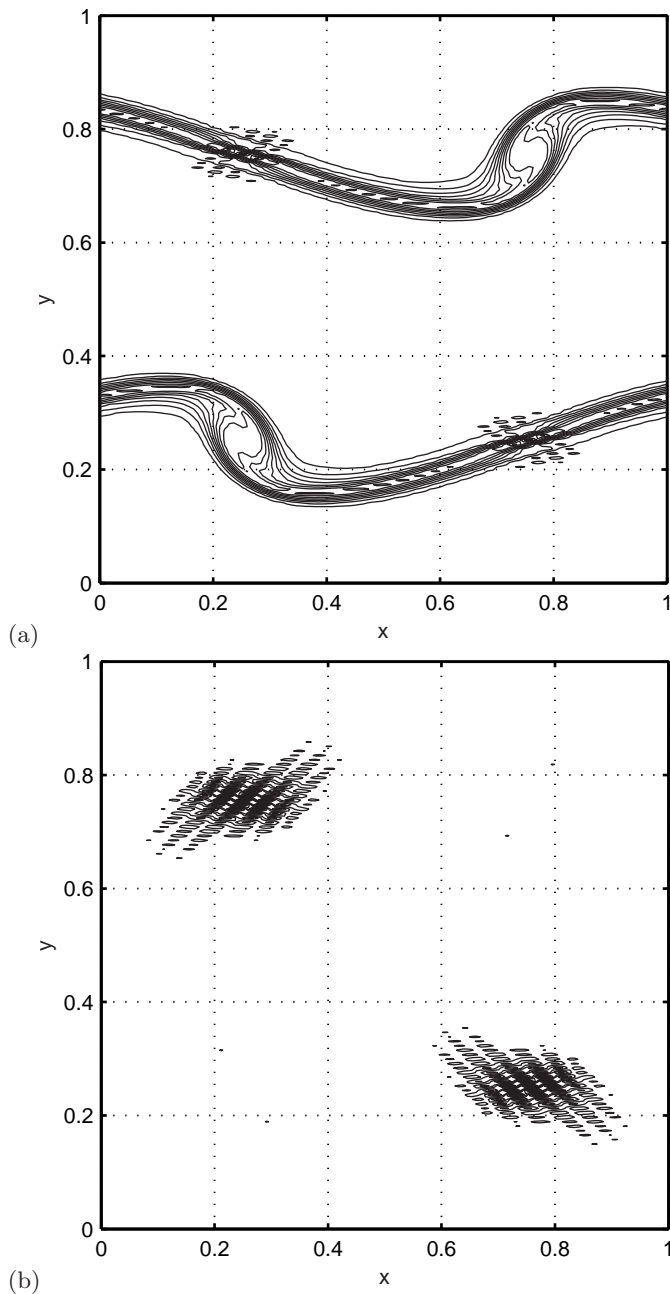


FIG. 3: Numerical vorticity (a) and divergence $\nabla \cdot \mathbf{u}$ (b) at $t = 0.6$ with parameters as in Fig. 2. The divergence was computed both spectrally from \mathbf{u} , and from $\text{Tr} \mathbf{\Pi}^{(1)}$ using (25). The peak divergence is 6% of the peak vorticity, and does not diminish as the Mach number is reduced from 0.04 to 0.01. Compare with Fig. 7 in [31]. The contour intervals are 6 and 0.5 respectively.

sistent treatment of the temperature. However the bulk viscosity's contribution to the deviatoric stress is readily adjusted, or removed altogether, by adding a term proportional to the local fluid divergence to the discrete equilibrium distribution. This divergence is available at each lattice point from the non-equilibrium parts of the distribution functions. Numerical experiments confirm

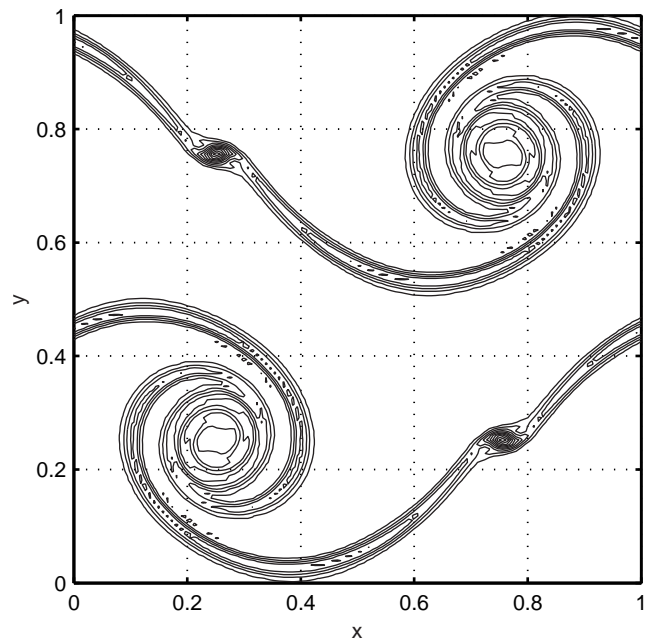


FIG. 4: Vorticity contours at $t = 1$. Stronger spurious vortices form in the absence of bulk viscosity, $\mu' = 0$. The contour interval is $\Delta\omega = 6$.

that sound waves experience the correct dissipation due to the intended bulk and shear viscosities. Deviations from the intended behaviour due to a finite mean free path, *i.e.* a finite Knudsen number, are no worse than in the unmodified lattice Boltzmann equation. An enhanced bulk viscosity of the order of $10 \leq \mu'/\mu \leq 100$ succeeded in suppressing spurious vortices created by an under-resolved nominally incompressible flow at high Reynolds number. This same modification could presumably be applied to other lattice Boltzmann schemes, such as the 17 speed scheme in [5]. Sensitivity to varying bulk viscosity may be a useful aid to identifying spurious features in under-resolved simulations of the kind found by Minion & Brown [31].

Acknowledgments

The author would like to thank John Hinch for commenting on a draft of this paper. Financial support from St John's College, Cambridge is gratefully acknowledged.

APPENDIX A: ANALYTICAL TREATMENT OF DECAYING SOUND WAVES

The viscous decay of sound waves may also be formulated as a linear eigenvalue problem of the kind considered in [32]. This resembles previous treatments of sound waves using the linearised continuum Boltzmann equation [14, 17]. We assume a distribution function of

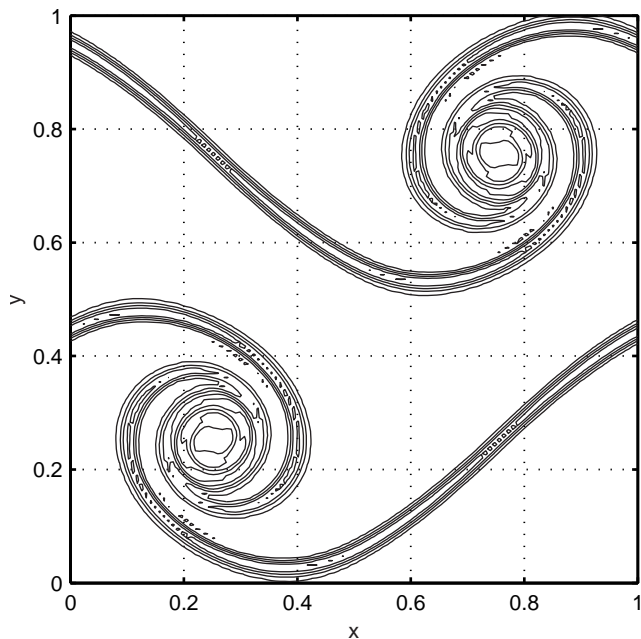


FIG. 5: Vorticity contours at $t = 1$. An enhanced bulk viscosity, $\mu' = 10\mu$, prevents the excessive thinning that leads to the formation of spurious vortices. An even larger bulk viscosity, $\mu' = 100\mu$, produced indistinguishable results. The contour interval is $\Delta\omega = 6$.

the form

$$\bar{f}_i(x, t) = F_i^{(0)} + h_i e^{ikx + \sigma t}, \quad (\text{A1})$$

where $F_i^{(0)}$ is the equilibrium distribution for a rest state with density ρ_0 , and the h_i are small unknown constants. This describes a small amplitude sound wave with complex frequency σ and wavenumber k propagating in the x -direction. The linearised fully discrete lattice Boltzmann equation, (40) with $f_i^{(0)}$ given by (43), then reduces to an eigenvalue problem of the form

$$h_i e^{ikc_i \Delta x + \sigma \Delta t} = h_i - \gamma \left(h_i - (f_i^{(0)} - F_i^{(0)}) \right), \quad (\text{A2})$$

for σ and the eigenvector h_i . The constant $\gamma = \Delta t / (\tau + \Delta t / 2)$. The term $f_i^{(0)} - F_i^{(0)}$ is a function of $\{h_0, \dots, h_8\}$ because $f_i^{(0)}$ depends on $\rho = \rho_0 + \sum h_j$ and $\rho \mathbf{u} = \sum \xi_j h_j$. This function may be taken to be linear when the h_i are sufficiently small.

The resulting 9×9 matrix eigenvalue problem is not analytically tractable, but a numerical evaluation of the eigenvalues gives excellent agreement with the measured decay rate of sound waves in the time dependent system, as shown in Fig. 6. This analysis also confirms that the deviations from the intended viscosity seen in Fig. 1 are functions of τ only, and thus of the combined parameter Ma/Re . The parabolic behaviour of the relative decay rate for small τ , as shown in Fig. 1, may be captured through a perturbation expansion of the eigenvalues, which may be found exactly for $\tau = 0$, carried up to

$O(\tau^3)$. These results are shown as dotted lines in Fig. 6. As usual, the higher order effects leading to the Burnett and super-Burnett equations improve the agreement for small τ , at least in a periodic domain where the question of boundary conditions for the higher order differential operators is straightforward, but do not provide a useful description for $\tau = O(1)$ [15, 32].

In the purely one dimensional case, using the three speeds $\xi_i = \{-1, 0, 1\}$ and weights $w_i = \{1/6, 2/3, 1/6\}$ respectively, the resulting eigenvalue problem for the modified system (40) is identical to that for the unmodified system with the same effective viscosity $(4/3)\nu + \nu'$. The matrix is

$$\frac{1}{3} \begin{pmatrix} (3 - \gamma)\Omega & \gamma\Omega/2 & -\gamma\Omega \\ 2\gamma & 3 - \gamma & 2\gamma \\ -\gamma/\Omega & \gamma/(2\Omega) & (3 - \gamma)/\Omega \end{pmatrix}, \quad (\text{A3})$$

where $\Omega = \exp(2\pi i/M)$ for a lattice with M points, and $\gamma = \Delta t / (\tau + \Delta t / 2)$ as in (A2). Thus the finite τ behaviour of the three speed one dimensional scheme with variable bulk viscosity is precisely the same as for the unmodified scheme with the same effective viscosity.

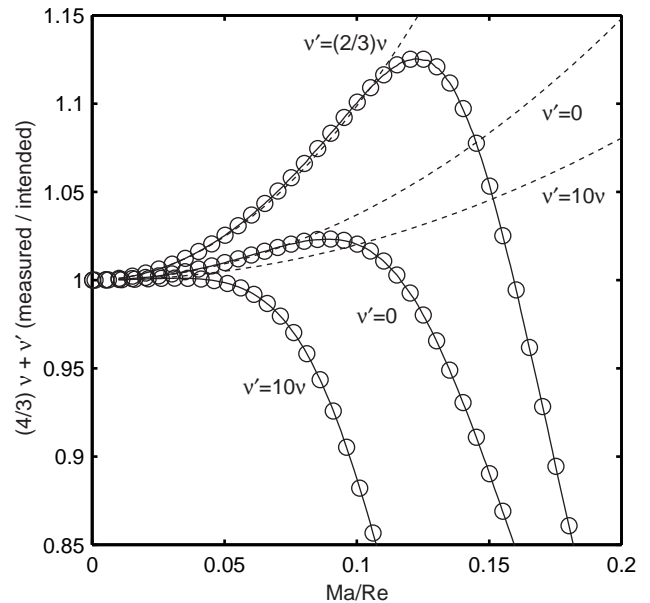


FIG. 6: Ratio of measured to intended effective viscosity $(4/3)\nu + \nu'$ for sound waves, plotted against Knudsen number $\text{Kn} = \text{Ma}/\text{Re} = \tau/\sqrt{3}$. Solid lines are from numerical experiments with decaying sound waves, as in Fig. 1, and the circles are from the eigenvalue formulation in the appendix. The dashed lines are the $O(\tau^3)$ behaviour from a small τ approximation to the eigenvalues. The unmodified 9 speed lattice Boltzmann scheme is equivalent to $\nu' = (2/3)\nu$ (uppermost curve).

-
- [1] S. Chen and G. D. Doolen, *Lattice Boltzmann method for fluid flows*, *Annu. Rev. Fluid Mech.* **30**, 329 (1998).
- [2] P. L. Bhatnagar, E. P. Gross, and M. Krook, *A model for collision process in gases. I. Small amplitude processes in charged and neutral one-component system*, *Phys. Rev.* **94**, 511 (1954).
- [3] Y.-H. Qian and S. A. Orszag, *Lattice BGK models for the Navier–Stokes equation – nonlinear deviation in compressible regimes*, *Europhys. Lett.* **21**, 255 (1993).
- [4] Y. Chen, H. Ohashi, and M. Akiyama, *Thermal lattice Bhatnagar–Gross–Krook model without nonlinear deviations in macrodynamic equations*, *Phys. Rev. E* **50**, 2776 (1994).
- [5] Y.-H. Qian and Y. Zhou, *Complete Galilean-invariant lattice BGK models for the Navier–Stokes equation*, *Europhys. Lett.* **42**, 359 (1998), also [ICASE Report TR-98-38](#), Institute for Computer Applications in Science and Engineering, NASA Langley Research Center.
- [6] J. D. Sterling and S. Chen, *Stability analysis of lattice Boltzmann methods*, *J. Comput. Phys.* **123**, 196 (1996), [arXiv:comp-gas/9306001](#).
- [7] D. J. Tritton, *Physical Fluid Dynamics* (Oxford University Press, Oxford, 1988), 2nd ed.
- [8] K. Huang, *Statistical Mechanics* (Wiley, New York, 1987), 2nd ed.
- [9] L. D. Landau and E. M. Lifshitz, *Fluid Mechanics* (Pergamon, Oxford, 1987), 2nd ed.
- [10] K. Stewartson, *The Theory of Laminar Boundary Layers in Compressible Fluids* (Oxford University Press, Oxford, 1964).
- [11] L. Rosenhead *et al.*, *A discussion on the first and second viscosities of fluids*, *Proc. Roy. Soc. Lond. A* **226**, 1 (1954).
- [12] G. K. Batchelor, *An Introduction to Fluid Dynamics* (Cambridge University Press, Cambridge, 1967).
- [13] H. Lamb, *Hydrodynamics* (Cambridge University Press, Cambridge, 1932), 6th ed.
- [14] C. Cercignani, *The Boltzmann Equations and its Applications* (Springer-Verlag, New York, 1988).
- [15] S. Chapman and T. G. Cowling, *The Mathematical Theory of Non-Uniform Gases* (Cambridge University Press, Cambridge, 1991), 3rd ed.
- [16] S. T. Choh, *The Kinetic Theory of Phenomena in Dense Gases*, Ph.D. thesis, The University of Michigan. (1958).
- [17] G. E. Uhlenbeck and G. W. Ford, *Lectures in Statistical Mechanics*, vol. 1 of *Lectures in Applied Mathematics* (American Mathematical Society, Providence, 1963).
- [18] S. Hou, Q. Zou, S. Chen, G. D. Doolen, and A. C. Cogley, *Simulation of cavity flow by the lattice Boltzmann equation*, *J. Comput. Phys.* **118**, 329 (1995), [arXiv:comp-gas/9401003](#).
- [19] P. J. Dellar, *A priori derivation of lattice Boltzmann equations for rotating fluids*, Submitted to *Phys. Rev. E* (2000).
- [20] U. Frisch, B. Hasslacher, and Y. Pomeau, *Lattice-gas automata for the Navier–Stokes equations*, *Phys. Rev. Lett.* **56**, 1505 (1986).
- [21] G. McNamara and G. Zanetti, *Use of the Boltzmann equation to simulate lattice-gas automata*, *Phys. Rev. Lett.* **61**, 2332 (1988).
- [22] H. Chen, S. Chen, and W. H. Matthaeus, *Recovery of the Navier–Stokes equations using lattice-gas Boltzmann method*, *Phys. Rev. A* **45**, R5339 (1992).
- [23] X. He and L.-S. Luo, *A priori derivation of the lattice Boltzmann equation*, *Phys. Rev. E* **55**, R6333 (1997).
- [24] X. He and L.-S. Luo, *Theory of the lattice Boltzmann method: From the Boltzmann equation to the lattice Boltzmann equation*, *Phys. Rev. E* **56**, 6811 (1997).
- [25] T. Abe, *Derivation of the lattice Boltzmann method by means of the discrete ordinate method for the Boltzmann equation*, *J. Comput. Phys.* **131**, 241 (1997).
- [26] X. Shan and X. He, *Discretization of the Velocity Space in the Solution of the Boltzmann equation*, *Phys. Rev. Lett.* **80**, 65 (1998), [arXiv:comp-gas/9712001](#).
- [27] P. J. Davis and P. Rabinowitz, *Methods for Numerical Integration* (Academic, New York, 1984), 2nd ed.
- [28] X. He, X. Shan, and G. D. Doolen, *Discrete Boltzmann equation model for nonideal gases*, *Phys. Rev. E* **57**, R13 (1998).
- [29] J. M. Buick, C. L. Buckley, C. A. Greated, and J. Gilbert, *Lattice Boltzmann BGK simulation of nonlinear sound waves: the development of a shock front*, *J. Phys. A* **33**, 3917 (2000).
- [30] Y.-H. Qian and Y. Zhou, *Higher-order dynamics in lattice-based models using the Chapman–Enskog method*, *Phys. Rev. E* **61**, 2103 (2000).
- [31] M. L. Minion and D. L. Brown, *Performance of under-resolved two-dimensional incompressible flow simulations, II*, *J. Comput. Phys.* **138**, 734 (1997).
- [32] P. Lallemand and L.-S. Luo, *Theory of the lattice Boltzmann method: Dispersion, dissipation, isotropy, Galilean invariance, and stability*, *Phys. Rev. E* **61**, 6546 (2000), also [ICASE Report TR-2000-17](#), Institute for Computer Applications in Science and Engineering, NASA Langley Research Center.